Simulation of Ship Motion in Seaway

by

Tristan Pérez † and Mogens Blanke‡

Technical Report EE02037

Dept. of Electrical and Computer Engineering
The University *of* Newcastle, NSW, 2308, Australia

‡Section of Automation at Ørsted.DTU
Technical University of Denmark, Building 326
DK-2800 Kgs. Lyngby, Denmark

Abstract

Accurate modelling and simulation of ship motion in seaway is essential to test applications of ship motion control strategies. In this report, we review the mathematical description of ocean waves, and their effect on the motion of marine vehicles. We present a simple method suitable for accurate simulation that incorporates parameters related to the recommended spectral family and particular vehicle being considered. Based on this method, we also present a simple algorithm to tune the commonly used shaping filters to model wave induced motion. This allows different simulation scenarios to be identified with given sea states and particular sailing conditions.

Introduction

Automatic control strategies for marine vehicles and structures are designed to improve their functions with adequate reliability and economy. It is essential to the design and development of such strategies that accurate and relatively simple mathematical models be available to describe the loads exerted and the motions of vehicles. On one extreme, the state of the art in maneuvering simulation of marine vehicles incorporates sophisticated models to describe the motion of the ship in different environments. These models are based on free-running model tests data, databases, and numerical simulation based on Computational Fluid Dynamics Methods (CFDM)—see for example (Simonsen, 2000). These models are typically too complex to be used for testing control strategies. On the other extreme, the literature on marine control applications such as autopilot, dynamic positioning and rudder roll stabilization, report very simple models utilized to design the control control algorithms. The latter models usually describe the sea state and the motion of the vessel by filtered white noise, *i.e.,* shaping filters. In this report, we review the description of ocean waves and propose a method to simulate ship motion in seaway that incorporates parameters related to the recommended spectral family and particular vehicle being considered. Then we present a simple algorithm to tune shaping filters that allows different simulation scenarios to be readily identified with given sea states and particular sailing conditions.

The rest of the report is organized as follows. In section 1, we introduce the stochastic mathematical models for describing sea states, and their properties. In section 2, we describe the relations between the sea elevation and ship motion components giving a stochastic mathematical description of the phenomena. In section 3, we present a simple algorithm to tune shaping filters and we show some simulation results. Finally, in section 4, we summarize and discuss the presented material.

1 Stochastic description of irregular seas

Ocean waves are random in terms of both time and space. Therefore, a stochastic modelling description seems to be the most appropriate approach to describe them—see for example St Denis and Pierson (1953).

In practice, it is assumed that the variations of the stochastic characteristics of the sea are much slower than the variations of the sea surface itself. Due to this, the elevation of the sea at a position x, y, denoted by $\zeta(x, y, t)$, can be considered a realization of a stationary process. The following simplifying assumptions about the underlying stochastic model are usually made (Haverre and Moan, 1985):

- The observed sea surface, at a certain location and for short periods of time, is considered a realization of a stationary and homogeneous, zero mean Gaussian stochastic process.
- Some standard formulae for the spectral density function $S(\omega)$ are adopted.

Under a Gaussian assumption, the process, in a statistical sense, is completely characterized by the power spectral density function $S(\omega)$.

The validity of this hypothesis of stationarity and Gaussianity, have been investigated via extensive analysis of time series recorded from wave riding buoys in the North Atlantic Ocean Haverre and Moan (1985). In this study, It has been reported that:

- For low and moderate sea states (Significant wave height[1] $h_{1/3} < 4m$), the sea can be considered stationary for periods over 20 min. For more severe sea states, stationarity can be questioned even for periods of 20 min.
- For low to medium states ($h_{1/3} < 8m$), Gaussian models are still accurate, but deviations from Gaussianity slightly increase with the increasing severity of the sea state.

Model to describe the sea elevation

A conceptual model to describe the elevation of an irregular sea is given by the sum of a large number of essentially independent regular (sinusoidal) contributions with random phases. In this representation, the sea elevation at a location x, y with respect to an inertial reference frame is given by

$$\zeta(x, y, t) = \sum_{i=0}^{N} \zeta_i(x, y, t) = \sum_{i=0}^{N} \overline{\zeta}_i \cos\left(k_i x \cos\chi + k_i y \sin\chi + \omega_i t + \theta_i\right), \tag{1}$$

where $\zeta_i(x, y, t)$ is the contribution of the regular or harmonic travelling wave components i progressing at an angle χ with respect to the inertial frame and a with random phase θ_i. The parameters k_i (wave number), ω_i (wave frequency seen from a fixed position), $\overline{\zeta}_i$ (constant wave amplitude) characterize each component. For each realization, the phase θ_i of each components is chosen to be a random variable with uniform distribution on the interval $[-\pi, \pi]$. This choice ensures the stationarity of $\zeta(x, y, t)$ (Gelb and Velde, 1968).

For each regular wave component i, the phase velocity, c_i, is the velocity with which the wave crest move relative to ground. Assuming infinite depth of water, the following relations hold

$$c_i = \sqrt{\frac{g\lambda_i}{2\pi}}; \quad k_i = \frac{2\pi}{\lambda_i}; \quad \omega_i = \sqrt{gk_i} = \frac{g}{c_i} \tag{2}$$

where λ_i is the wavelength of the component i. The last expression is known as the dispersion of gravity waves, and establishes that the phase velocity is inversely proportional to its frequency. This means that long waves propagate faster than short ones. This phenomenon is important for simulating ship motion in waves as we shall see in the following sections of the report: a ship advancing in a seaway in following seas will overtake some short waves, while it will be overtaken by some long ones.

For simplicity, let us consider the case in which the observations are made at the origin of the reference

[1] The significant wave height $h_{1/3}$ is related to the wind speed and it is defined as the average of one third of the highest observations of the wave amplitude (Price and Bishop, 1974), *i.e.*, $h_{1/3} \triangleq \frac{3\sum \text{Highest one third of the sampled waves}}{\text{Total number of sampled waves}}$.

frame, and that the waves come from angle of incidence $\chi = 0$ with respect to the reference frame. The amplitude of the wave components, is then conveniently defined in terms of a adopted local power spectral density $S(w)$ satisfying

$$\text{var}[\zeta(t)] = \int_0^\infty S(\omega) d\omega. \tag{3}$$

Thus, for the case considered, the model of the seas elevation (1) becomes

$$\zeta(t) = \sum_{i=0}^{N} \zeta_i(t) = \sum_{i=0}^{N} \overline{\zeta}_i \cos(\omega_i t + \theta_i), \tag{4}$$

where at any particular wave frequency ω_i, the variance of that component within a band Δ_ω centered at ω_i is approximated by

$$\text{var}[\zeta_i(t)] = \frac{1}{2}\overline{\zeta_i}^2 \approx \int_{\omega_i - \frac{\Delta_\omega}{2}}^{\omega_i + \frac{\Delta_\omega}{2}} S(\omega) d\omega. \tag{5}$$

The amplitudes of wave components can be approximated by

$$\overline{\zeta_i} \approx \sqrt{2 \int_{\omega_i - \frac{\Delta_\omega}{2}}^{\omega_i + \frac{\Delta_\omega}{2}} S(\omega) \quad d\omega}. \tag{6}$$

Recommended spectra for fully-developed long-crested seas

In any particular sea state, the elevation of the ocean surface presents irregular characteristics. After the wind has blown constantly for a certain period of time the sea elevation becomes statistically stable. In this case, the sea is referred to as *fully-developed*. If the irregularity of the observed waves are only in the dominant wind direction so that there are mainly uni-directional wave crests with varying separation and remaining parallel to each other the sea is referred to as a *long-crested* irregular sea (Price and Bishop, 1974).

Based on extensive data collection, mostly in the North Atlantic ocean, a series of idealized single side local spectra have been obtained to described long-crested seas. For example, for fully-developed seas the one-parameter Pierson-Moskowits (PM) spectrum is given by—see for example (Price and Bishop, 1974):

$$S_{\text{PM}}(\omega) = \frac{0.78}{\omega^5} \exp\left(\frac{-3.11}{\omega^4 \; h_{1/3}^2}\right) \qquad (m^2 sec), \tag{7}$$

in which the main parameter is the significant wave height, $h_{1/3}$. The peak frequency of the PM spectrum is

$$\omega_0 = 1.26 \; h_{1/3}^{-1/2}. \tag{8}$$

For prediction of the responses of marine vehicles and offshore structures, The 2nd International Ship and Offshore Structures Congress (ISSC, 1964) and 12th and 15th International Towing Tank Conference (ITTC, 1969, 1978) recommended the use of a Modified Pierson-Moskowits (MPM) spectrum. When SI units are used, this has the form:

$$S_{\text{MPM}}(\omega) = \frac{4\pi^3 h_{1/3}^2}{\omega^5 T^4} \exp\left(\frac{-16\pi^3}{\omega^4 T^4}\right) \qquad (m^2 sec), \tag{9}$$

in which the main parameters are the significant wave height, $h_{1/3}$ and the dominant wave period T. The period corresponding to peak frequency of the spectrum is given by

$$T_0 = 1.408 \quad T. \tag{10}$$

This spectrum should be used to simulate fully developed seas with infinite depth, no swell and unlimited fetch[2] (Fossen, 1994). For cases in which geographical boundaries limit the fetch, the so-called JONSWAP (Join North Sea Wave Project) is recommended—see for example, (Lewis, 1988), (Faltinsen, 1990) and references therein.

[2] *Fetch* is the distance between the point at which the waves are observed and a windward boundary, such as a shore or the edge of a storm area. The fetch gives a notion of the area of interaction between the wind and sea surface with respect to the observation point.

Figure 1 shows the form of PM and MPM spectra for different significant wave heights. The significant wave height can be larger than 2m for 60% of the time in hostile areas such as the North Sea and reach 20m in extreme conditions with average winds over 60kts (Price and Bishop, 1974). The mean period can be between 4sec and 20sec, but is usually not below that (Faltinsen, 1990). Figure 2 shows the value of the

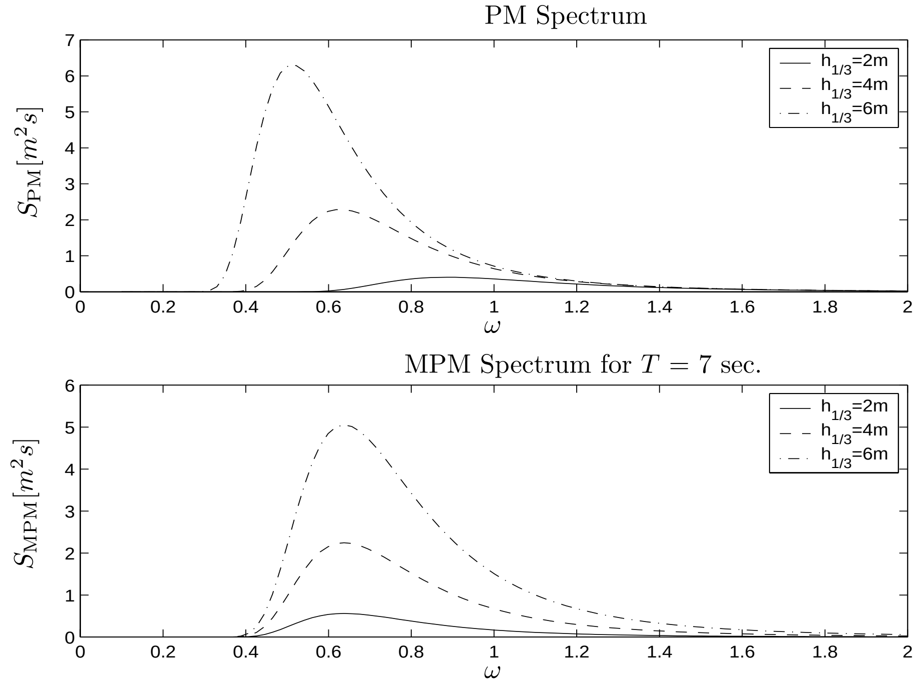

Figure 1: PM spectrum and recommended MPM by ITTC and ISSC for different significant wave height $h_{1/3}$.

regular amplitude components calculated using (6) for MPM spectrum for a given vector of frequencies. This figure also shows a particular realization of the sea elevation $\zeta(t)$ determined using (4) with a vector of random phases uniformly distributed on $[-\pi, \pi]$.

Short-crested seas

When irregularities are apparent along the wave crests at right angles to the direction of the wind, the sea is referred to as *short-crested* irregular sea or *confused* sea (Price and Bishop, 1974). Short-crestedness is characteristic of locations closer to storm areas due to the angular dispersion or spreading of many wave systems coming from different directions. In a short-crested sea, the waves approach the vessel or marine structure from a variety of directions χ with a main direction of propagation χ_0. For this case, a directional spectrum taking into account the different directions of the components gives a more accurate description. The elevation of the sea surface is then described by,

$$\zeta(t) = \sum_{i=0}^{N} \sum_{j=0}^{M} \overline{\zeta}_{ij} \cos[-\omega_i t + \theta_{ij}] \tag{11}$$

where,

$$\mathrm{var}[\zeta(t)] = \int_0^{\infty} \int_{-\pi}^{\pi} S(\omega, \alpha) d\alpha d\omega. \tag{12}$$

In which, $S(\omega, \alpha)$ is a so-called directional or two-dimensional spectrum (Price and Bishop, 1974), with $\alpha \triangleq \chi - \chi_0$, and

$$\overline{\zeta}_{ij} \approx \sqrt{2S(\omega_i, \alpha_j)\Delta_\alpha \Delta_\omega}. \tag{13}$$

Since the measurement of directional spectra is, in general, very difficult, in most applications, it is sufficient to assume that $S(\omega, \alpha)$ can be factorized as $S(\omega, \alpha) = S(\omega)M(\alpha)$. The factor $M(\alpha)$ is called the spreading

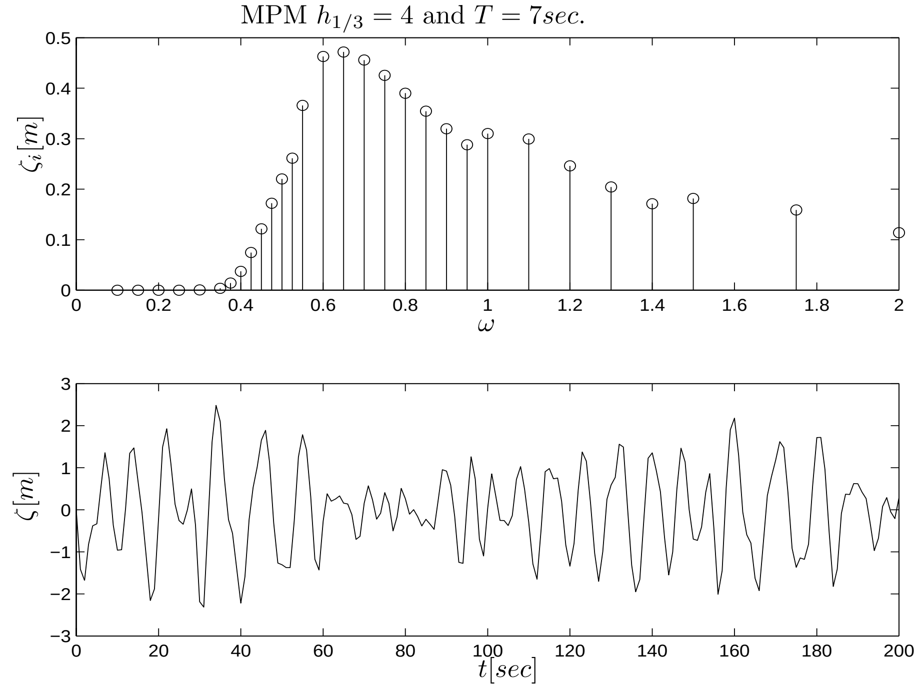

Figure 2: Amplitude of regular wave components ζ_i calculated using MPM with $h_{1/3} = 4$ and $T = 7sec$, and a particular realization. height $h_{1/3}$.

function. The usually adopted (and recommended by ITTC) spreading function is given by

$$M(\alpha) = \begin{cases} \frac{2\cos^2(\alpha)}{\pi} & \text{if } -\pi/2 \leqslant \alpha \leqslant \pi/2, \\ 0 & \text{otherwise.} \end{cases} \tag{14}$$

2 Ship motion in Seaway

The response of a ship to waves is very complex. Having a certain velocity of advance, a ship experiences the wave excitation at an encounter frequency. As we will see, this frequency is not related linearly to the wave frequency, as seen from a fixed point, but varies with ship speed and predominant direction between waves in a nonlinear fashion.

Frequency of encounter and encounter wave spectra

The sea state description from the ship is affected significantly by a doppler shift in the component frequencies of the wave pattern. If we assume a body-fixed frame oriented in such a way that the x_0-axis coincides with the fixed reference frame x-axis, and the ship moving with a forward speed U_0—see figures 3. Then, the relation between the two reference frames is given by

$$\begin{aligned} x &= x_0 + U_0 t \\ y &= y_0. \end{aligned} \tag{15}$$

Substituting these equations into the expression of a regular wave component, and considering a fixed direction χ—see figure 4, a regular wave component seen from the ship becomes

$$\zeta\,(x_0, y_0, t) = \zeta_0 \cos\left[k(x_0 \cos\chi + y_0 \sin\chi) - (\omega - kU_0 \cos\chi)t + \theta\right], \tag{16}$$

where the coefficient multiplying t is defined as the frequency of encounter, *i.e.,*

$$\omega_e = \omega - \frac{\omega^2 U_0 \cos\chi}{g}, \tag{17}$$

in which we have substituted the value of the wave number k using the relationships given in (2). Since the energy of the encounter waves is the same as that of the waves defined with respect of the fixed axes (the energy does not change if the point of observation changes) we have

$$\int_0^\infty S(\omega)d\omega = \int_0^\infty S(\omega_e)d\omega_e, \tag{18}$$

where

$$S(\omega)d\omega = S(\omega_e)d\omega_e. \tag{19}$$

Therefore, from (17), it follows that spectrum observed by the ship is then given by

$$S(\omega_e, \chi) = \frac{S(\omega, \chi)}{|1 - (2\omega U_0/g)\cos\chi|}. \tag{20}$$

Once the encounter wave spectrum has been obtained, it is necessary to relate it to the motion of the ship. To do this, there are two approaches. Both methods are based upon the simplifying assumption that the motion response of the ship is linear with respect to the wave amplitude in regular waves, *i.e.,* superposition holds. The first approach consists of approximating the forces and moments generated by each regular component using formulas for a rectangular parallelepiped and include this terms in the equations of motion as proposed by Källström (1979). The second approach uses the so-called Amplitude Response Operators (RAO) and relates the sea elevation to the particular motion component under consideration. In this method, the forces and moments are integrated over the wetted surface taking into account the load conditions, the geometry of the hull and the sailing conditions. It has been reported that the second method approximates the response of the vessel more accurately than the fist method (Blanke, 1981). In the sequel, we follow the second approach.

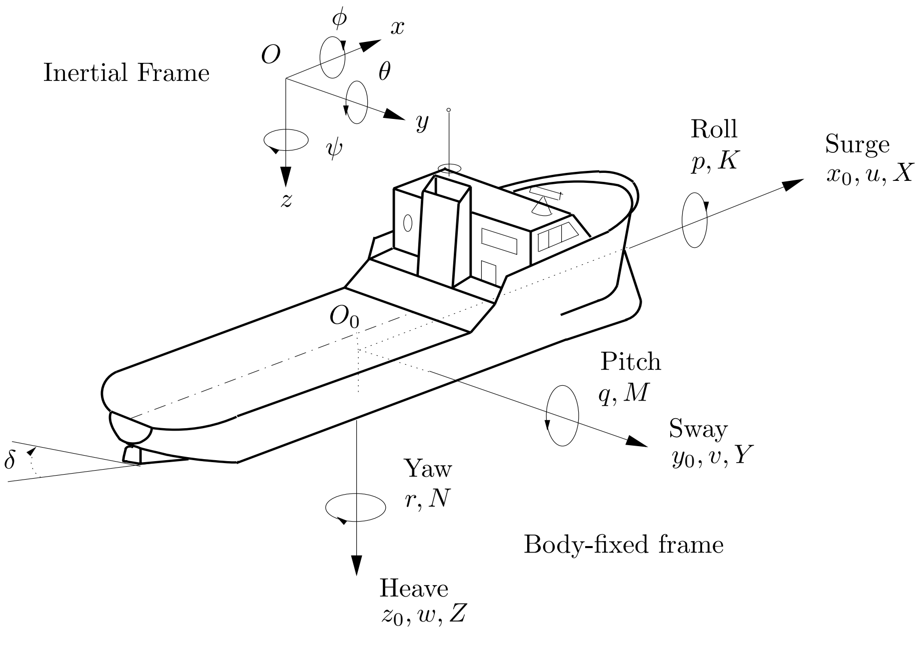

Figure 3: Standard notation and sign conventions for ship motion description (SNAME, 1950).

Response operators

The relationship between ship motion and wave height versus regular wave frequency is commonly called the Response Amplitude Operators (RAO) (Lewis, 1988). This relationship represents a linear approximation of the frequency response of the ship motion in regular waves. Under the linearity assumption, superposition can be applied to determine the motion of the ship; and therefore, a connection to the stochastic model for describing irregular waves given in the previous section can be established.

The RAO depend on the geometry of the hull and load conditions of the vessel as well as its speed and

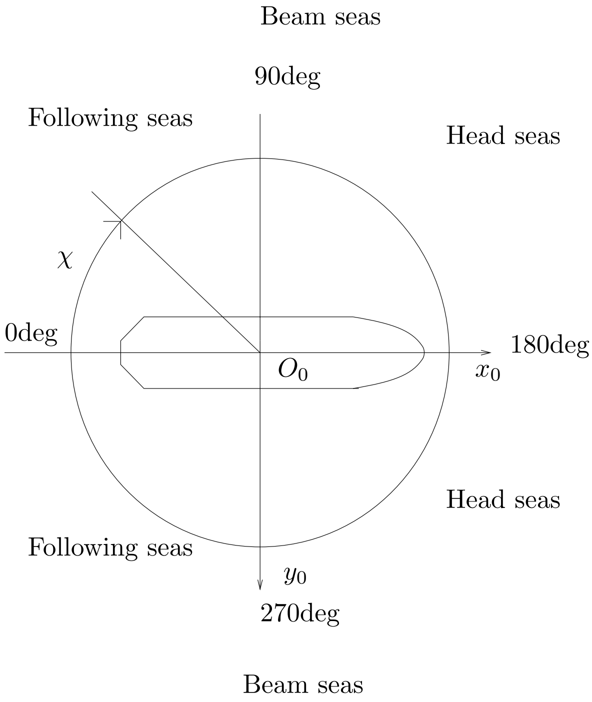

Figure 4: Definition of Encounter angle χ and sailing conditions.

direction with respect of the waves. The motion of a ship in six degrees of freedom is considered as a traslation motion (position) in three directions: surge, sway, and heave; and as a rotation motion (orientation) about three axis: roll, pitch and yaw—see figure 3. To determine the equations of motion, two reference frames are considered: the inertial or fixed to earth frame O that may be taken to coincide with the ship-fixed coordinates in some initial condition and the body-fixed frame O_0—see figure 3. For surface ships, the most commonly adopted position for the body-fixed frame is such it gives hull symmetry about the x_0z_0-plane and approximate symmetry about the y_0z_0-plane. The origin of the z_0 axis is defined by the calm water surface (Price and Bishop, 1974).

The magnitudes describing the position and orientation of the ship are usually expressed in the inertial frame and the coordinates are noted: $[x \quad y \quad z]^{\mathrm{T}}$ and $[\phi \quad \theta \quad \psi]^{\mathrm{T}}$ respectively— see figure 3. We have used the standard notation given in SNAME (1950).

Let us define the position-orientation vector η expressed in the inertial frame as

$$\eta \triangleq \begin{bmatrix} x & y & z & \phi & \theta & \psi \end{bmatrix}^{\mathrm{T}} \tag{21}$$

The RAO from the sea elevation ζ to a motion component η_i of η will be denoted

$$R_{\eta_i\zeta}(\omega_e, \chi, U) = |R_{\eta_i\zeta}(\omega_e, \chi, U)| \angle \arg(R_{\eta_i\zeta}(\omega_e, \chi, U)), \tag{22}$$

where the encounter angle χ is defined as zero astern and positive towards the port side of the vessel—see figure 4. For a particular load condition, encounter angle χ and speed U, the RAO are determined using strip theory computations in which the forces and moments are integrated over the wetted surface of the hull. The RAO are usually tabulated as function of the wave frequency instead of encounter frequency. To transform the RAO to encounter frequency, we simply have to use the transformation given in (17). For example, figure 5 shows the RAO corresponding to roll motion of a multi-role naval vessel (Blanke and Christensen, 1993)[3] as a function of the wave frequency ω.

The motion spectrum is then given by

[3]These RAO have been adapted from another ship by the authors to have a complete model for simulation purposes. The real RAO for this naval vessel are not available for publication.

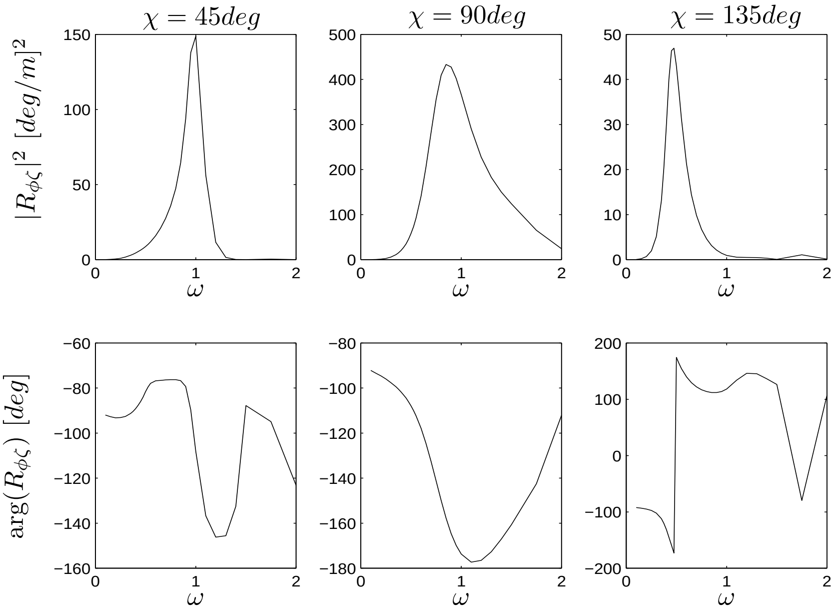

Figure 5: RAO of roll motion for a multi-role naval vessel at 18.5kts.

$$S_{\eta_i\eta_i}(\omega_e, \chi, U) = |R_{\eta_i\zeta}(\omega_e, \chi, U)|^2 S(\omega_e, \chi), \tag{23}$$

where $S(\omega_e, \chi)$ is given in (20).

Simulation of Ship motion

To simulate the motion of a ship given the motion spectrum, we can proceed in a similar manner as we did to simulate the elevation of the sea surface, *i.e.,* as a finite sum of sinusoidal components with a random initial phase:

$$\eta_i(t) = \sum_{k=1}^{N} \overline{\eta_{ik}} \cos(\omega_{ek} t + \theta_k). \tag{24}$$

The use of (23) to obtain the amplitudes $\overline{\eta_{ik}}$ of the corresponding regular sea components is involved since the inverse of the non-linear transformation (17) is multi-valued in some cases and (23) is almost singular at some frequencies. This is illustrated in the following example.

A numerical example for the transformation between the wave frequency ω and the observed frequency ω_e (*cf.,* (17)) is shown in figure 6. In this example the forward speed is $U = 9$m/sec (18.5kts), and $\omega \in [0.1, 2]$rad/sec. When sailing in beam seas, ($\chi = 90$deg or $\chi = 270$deg), ω and ω_e are the same since $\cos(\chi) = 0$ (*cf.,* (17)). When sailing in head seas (90deg $< \chi <$ 270deg) there is an effect of increase in the observed frequency. When sailing in following seas (270deg $< \chi$and$\chi <$ 90deg), there is a folding effect and three bands of different wave frequencies are mapped into a single band of encounter frequencies. Figure 6 shows this for the case of $\chi = 45deg$. The contribution of the three different band of frequencies should be accounted for in the transformation of the motion spectra.

In addition to this, for some particular frequencies, the encounter spectrum obtained as (23) becomes almost singular and numerical problems arise. For example, following the same numerical example shown in figure 6, calculations indicate that for ω close to 0.77 rad/sec, the corresponding $S(\omega_e, \chi)$ will be almost singular since its denominator tends to zero (*cf.,* (20)). To avoid these inconveniences, we can approximate the motion spectrum by using regular components given at particular frequencies as proposed by Blanke (1981), which we describe below.

The frequency of the individual components ω_{ek} in (24) are taken as the transformed frequencies at which the RAO have been computed and tabulated. Then, the amplitudes of the components in (24) are determined by

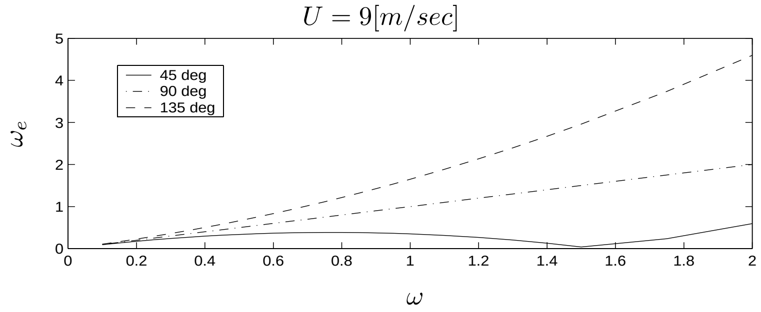

Figure 6: Transformation to frequency of encounter

integration from

$$\frac{1}{2}\overline{\eta_{ik}}^2 = \int_{\omega_{e1k}}^{\omega_{e2k}} S_{\eta_i\eta_i}(\omega_e)d\omega_e = \int_{\omega_{1k}}^{\omega_{2k}} |R_{\eta_i\zeta}(\omega_k,\chi,U)|^2 S(\omega,\chi)d\omega. \tag{25}$$

Therefore,

$$\overline{\eta_{ik}} = \sqrt{2|R_{\eta_i\zeta}(w_k,\chi,U)|^2 \int_{\omega_{1k}}^{\omega_{2k}} S(\omega,\chi)d\omega}, \tag{26}$$

where

$$\omega_{1k} = \omega_k - \Delta_{1k}; \qquad \omega_{2k} = \omega_k + \Delta_{2k} \tag{27}$$

$$\Delta_{1k} = (\omega_k - \omega_{k-1})/2; \qquad \Delta_{2k} = (\omega_{k+1} - \omega_k)/2. \tag{28}$$

Using this method, the components are calculated in the wave frequency domain instead of in the observed frequency domain. This procedure avoids the problem of that arises when the amplitudes of the regular components are calculated from a spectrum with infinite peaks.

Once the amplitudes of the components are obtained, we can simulate different realizations of the stochastic process using (24). As we will show in the following section, we can also approximately reconstruct the motion spectrum from the components.

Figure 7 shows the results obtained for roll motion of a multi-role naval vessel using the proposed method for different sea directions, and for an irregular sea described by MPM with parameters $h_{1/3} = 4$m and $T = 7$sec. These figure shows the amplitudes of the components and the corresponding time series of the roll motion. From figure 7, it is clear the doppler effect on the wave frequencies experienced on the ship. It is also worth noting, for this example the how the different frequencies are mapped in to ω_e for the case of encounter angle $\chi = 45$deg.

3 Shaping filters to approximate ship motion

A very simple model of the ship motion adopted to design and test control strategies is filtered white noise. The transfer function of the, generally, adopted filter is of the form

$$H(s) = \frac{Ks}{s^2 + 2\xi\omega_n s + \omega_n^2}. \tag{29}$$

The Power Spectral Density (PSD) of the particular motion component considered (roll, yaw, sway, *etc.*) is then approximated by

$$P_{\hat{\eta}_i\hat{\eta}_i}(\omega_e) = \frac{K^2\omega_e^2 P_n}{(\omega_n^2 - \omega_e^2)^2 + (2\xi\omega_n)^2\omega_e^2}, \tag{30}$$

where P_n is the intensity (power) of the white noise. If the gain in (29) is defined as $K \triangleq 2\xi\omega_n$, it follows from (30) that

$$\max_{\omega_e} P_{\hat{\eta}_i\hat{\eta}_i}(\omega_e) = P_{\hat{\eta}_i\hat{\eta}_i}(\omega_n) = P_n. \tag{31}$$

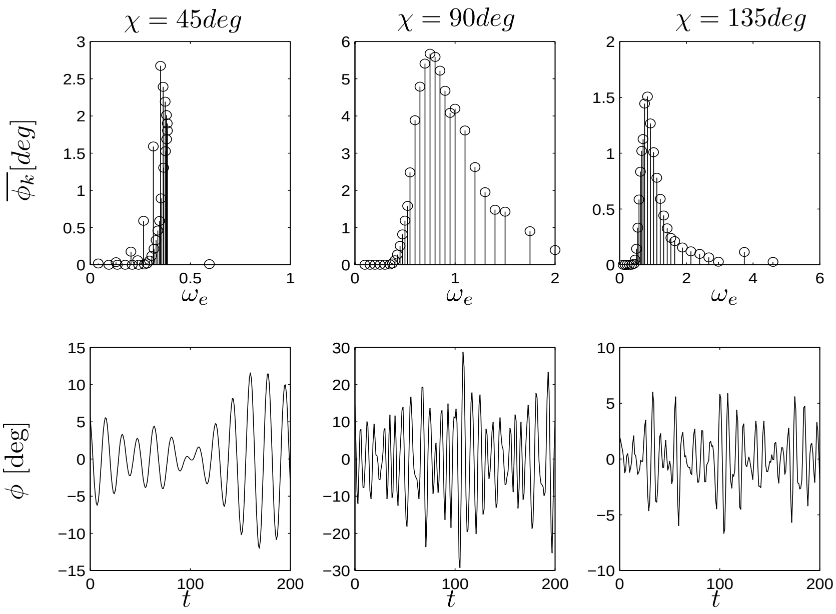

Figure 7: Roll motion for a multi-role naval vessel at 18.5kts in following seas using a MPM spectrum.

Todate, little has been reported in the literature on how to tune the shaping filters so as to describe accurately the behavior of the marine vehicle in seaway. For example, in (Rhee and Kim, 2000), a method using least square fitting was reported. However, this method gives unstable results in some cases. Therefore, in this section we propose a simple method to adjust the parameters of the shaping filters based on a discrete-frequency approximation of the motion psd.

To tune the parameters of this filter according to given sailing conditions, we first need to obtain a discrete frequency approximation of the PSD of the motion from the regular components of (24). This can be done by

$$P^*_{\eta_i\eta_i}(\omega_{ek}) \approx \frac{\pi\overline{\eta_{ik}}^2}{2\Delta_{\omega_{ek}}} \qquad \text{for} \quad k = 1, \ldots, N, \tag{32}$$

where $\Delta_{\omega_{e1}} \triangleq (\omega_{e2} - \omega_{e1})$, $\Delta_{\omega_{ek}} \triangleq (\omega_{e(k+1)} - \omega_{e(k-1)})/2$ for $k = 2, \ldots, N-1$ and $\Delta_{\omega_{eN}} \triangleq (\omega_{e(N)} - \omega_{e(N-1)})$.

Then given $P^*_{\eta_i\eta_i}(\omega_{ek})$, we propose the following rules for tuning the filter:

$$P_n = \max_{\omega_{ek}} P^*_{\eta_i\eta_i}(\omega_{ek}), \tag{33}$$

$$\omega_n = \arg\max_{\omega_{ek}} P^*_{\eta_i\eta_i}(\omega_{ek}), \tag{34}$$

The damping coefficient ξ_i is calculated so as to match the variance of the output of the filter $\hat{\eta_i}$ and the variance of η_i obtained by the realizations generated by (24). If the filter is expressed into a state space form

$$\begin{aligned} \dot{x}_f &= A_f(\xi)x_f + B_f w \\ \hat{\eta_i} &= C_f x_f. \end{aligned} \tag{35}$$

then, for a white noise w with power intensity P_n, the steady state variance of the output is given by

$$\mathrm{var}(\hat{\eta_i}) = C_f P_{x_f x_f} C_f^{\mathrm{T}}. \tag{36}$$

Where $P_{x_f x_f}$ is the covariance of the state x_f and satisfies the following Lyapunov equation:

$$A_f(\xi)P_{x_f x_f} + P_{x_f x_f}A_f(\xi)^{\mathrm{T}} + B_f P_n B_f^{\mathrm{T}} = 0. \tag{37}$$

Therefore, we seek ξ_i such that

$$C_f P_{x_f x_f} C_f^{\mathrm{T}} - \frac{1}{\pi}\sum_{k=0}^{N} P^*_{\eta_i\eta_i}(\omega_{ek}) = 0. \tag{38}$$

where the second term of the left hand side is an approximation of the variance of the motion component. This last equation can be solved for example using a bi-section algorithm.

To illustrate the the method, figure 8, shows an example for the multi-role naval vessel. The results were obtained using a MPM spectrum of significant wave height $h_{1/3}$ =4m and T =7sec and sailing conditions of U =9m/sec (18.5kts) and $\chi = 135deg$. The first plot shows the discrete frequency approximation of the PSD of the roll motion ($P^*_{\eta_i\eta_i}(\omega_{ek})$) and the PSD of the output of the filter ($P_{\hat{\eta}_i\hat{\eta}_i}(\omega_e)$). The second plot shows a times series generated using (24). The third plot shows the output of the tuned filter. The simulations gave var(ϕ) = 5.86 and var($\hat{\phi}$) = 5.50. Figure 9 shows similar results for following seas. For the latter case, the results are less accurate due to the folding effects.

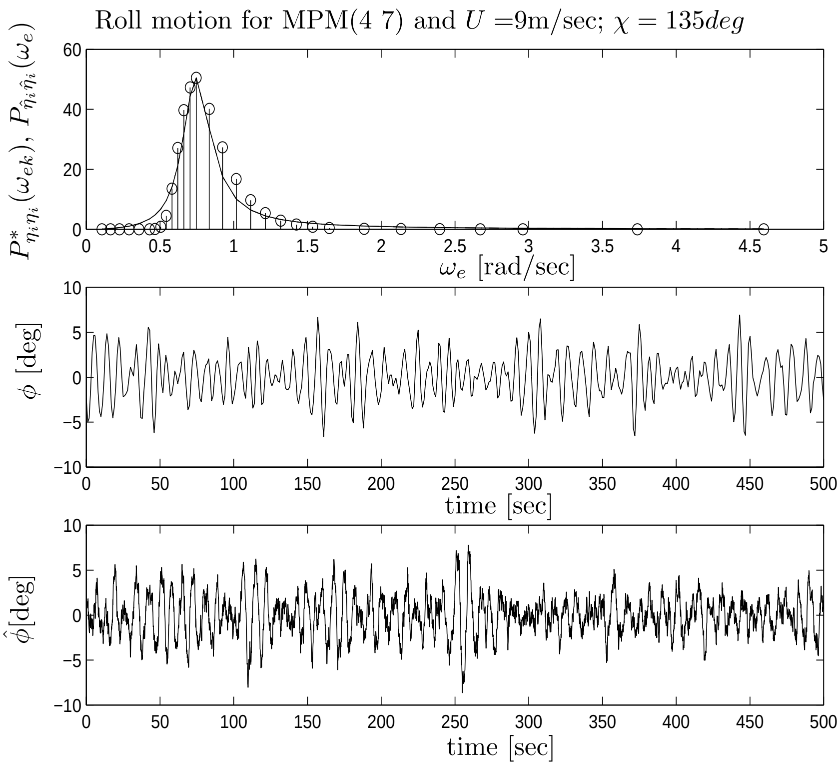

Figure 8: Roll motion for a multi-role naval vessel at 18.5kts in head seas.

The second order approximation gives very good results for the roll motion. However, to approximate other motion components better, higher order filters may be necessary. In those cases the filters may be fitted using regression.

4 Summary and discussion

It is a common practice in control design to use simple models as a first step towards the design of control strategies, and there is no exception in applications of motion control of marine systems. The simplest way to describe the motion of a marine vehicle is by using filtered white noise, *i.e.,* colored noise. However, little has been reported in the literature on how to tune the shaping filters so as to describe accurately the behavior of the marine vehicle in seaway. In this report, we have reviewed the modelling of ocean waves and presented a simple and accurate method to simulate the motion of marine vehicles in seaway based upon the RAO and particular sea states. Using this method, we have also presented a simple algorithm to tune shaping filters based upon a discrete-frequency approximation of the motion spectrum. A similar method can easily be implemented for discrete-time estimation based on records of motion components using discrete Fourier transform (FFT).

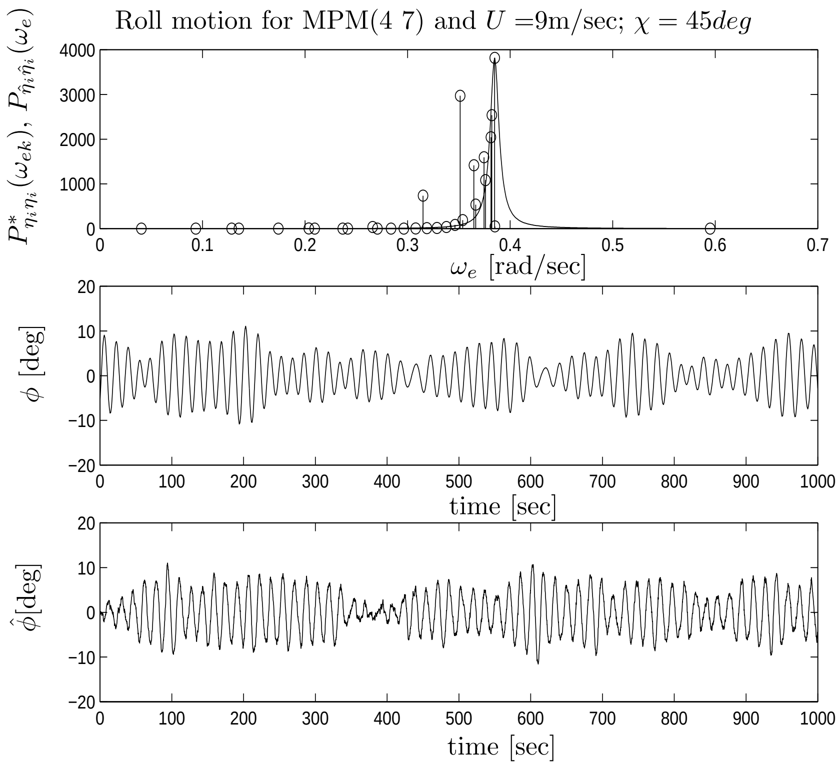

Figure 9: Roll motion for a multi-role naval vessel at 18.5kts in following seas.

Acknowledgements

The authors would like to thank Prof. Ching-Yaw Tzeng from Institute of Marine Technology at National Taiwan Ocean University, Taiwan, R.O.C. for his comments and also for providing the RAO presented in this work.

References

Blanke, M. (1981). Ship propulsion losses related to automatic steering and prime mover control. PhD thesis. Servolaboratory, Technical University of Denmark.

Blanke, M. and A. Christensen (1993). Rudder roll damping autopilot robustness to sway-yaw-roll couplings. *In: Proceedings of 10th SCSS, Ottawa, Canada* pp. 93–119.

Faltinsen, O.M. (1990). *Sea loads on ships and offshore strucutres.* Cambridge University Press.

Fossen, T.I. (1994). *Guidance and Control of Ocean Marine Vehicles.* John Wiley and Sons Ltd. New York.

Gelb, A. and W.E. Vander Velde (1968). *Multiple-input describing functions and nonlinear system design.* McGraw Hill.

Haverre, S. and T. Moan (1985). *On some uncertainties related to short term stochastic modelling of ocean waves.* In: Probabilistic Offshore Mechanics, Progress in Engineering Science, CML Publications Ltd.

Källström, C.G. (1979). Identification and Adaptive Control Applied to Ship Steering. PhD thesis. Lund Institute Of Technology, Lund, Sweden.

Lewis, E.V. (Ed.) (1988). *Principles of Naval Architecture vol III: Motions in Waves and Controllability.* 3rd ed.. Society of Naval Architects and Marine Engineers, New York.

Price, W. C. and R. E. D. Bishop (1974). *Probabilistic theory of ship dynamics.* Chapman and Hall, London.

Rhee, K.P. and S.H. Kim (2000). A modelling of frequency-dependent vertical ship motions in irregular waves. *Proc. 3rd International Conference for High Performance Marine Vehicles (HPMV 2000).*

Simonsen, C. D. (2000). Rudder, propeller and hull interaction by RANS. PhD thesis. Dept. of Naval Architecture and Offshore Eng., Technical University of Denmark.

SNAME (1950). Nomenclature for treating the motion of a submerged body through a fluid. Technical Report Bulletin 1-5. Society of Naval Architects and Marine Engineers, New York, USA.

St Denis, M. and W.J. Pierson (1953). On the motion of ships in confused seas. *SNAME Transactions.*